

Advances in the limits of separation power in supercritical fluid chromatography

Broeckhoven, Ken

Published in:
TrAC - Trends in Analytical Chemistry

DOI:
[10.1016/j.trac.2021.116489](https://doi.org/10.1016/j.trac.2021.116489)

Publication date:
2022

License:
CC BY-NC-ND

Document Version:
Accepted author manuscript

[Link to publication](#)

Citation for published version (APA):
Broeckhoven, K. (2022). Advances in the limits of separation power in supercritical fluid chromatography. *TrAC - Trends in Analytical Chemistry*, 146, [116489]. <https://doi.org/10.1016/j.trac.2021.116489>

Copyright

No part of this publication may be reproduced or transmitted in any form, without the prior written permission of the author(s) or other rights holders to whom publication rights have been transferred, unless permitted by a license attached to the publication (a Creative Commons license or other), or unless exceptions to copyright law apply.

Take down policy

If you believe that this document infringes your copyright or other rights, please contact openaccess@vub.be, with details of the nature of the infringement. We will investigate the claim and if justified, we will take the appropriate steps.

Highlights:

- The low viscosity of CO₂-based mobile phases allows high kinetic performance.
- To allow the use of high modifier content, higher operating pressures are required
- Improvements in extra-column dispersion needed to enable the use of narrow ID columns
- New chiral stationary phases allow very fast (<1min) enantioseparations
- Injection solvent effects deteriorate 1D and 2D performance of SFC.

Advances in the limits of separation power in Supercritical Fluid Chromatography

Ken Broeckhoven*

Vrije Universiteit Brussel, Pleinlaan 2, 1050 Brussel, Belgium

(*) Corresponding author: email: Ken.Broeckhoven@vub.be

tel.: ++3226293249 fax.: ++3226293248

Abstract

The use of CO₂-based mobile phases for separations, more generally referred to as supercritical fluid chromatography (SFC), allows to perform highly efficient and fast separations due to its low viscosity and high diffusivity of the solutes in the mobile phase. Nevertheless, the instrumental capabilities of current state-of-the art instrumentation in SFC is still not on the same level as that of ultra-high performance liquid chromatography. Not only is the maximum operating pressure lower, also the extra-column fluidic path is not fully optimized to exploit the possibilities of high efficiency columns packed with small particles. The effect of the strong solvent injection inherent to SFC hinders the optimal implementation of short small particle columns. The current limits in separation power in SFC are discussed and the requirements for future generation instruments are reviewed. An overview is presented of innovations in column technology, separation conditions and optimization of the instrumental design.

Keywords:

Supercritical Fluid Chromatography, unified chromatography, kinetic performance limits, extra-column band broadening, column technology

1. Introduction

The use of supercritical fluids as mobile phase has long been heralded as the ideal compromise between the superior separation speeds and efficiencies obtained in gas chromatography (GC) and the superior solute solubility in liquid chromatography (LC) where much higher density mobile phases are used. Although many fluids can be used in their supercritical state, supercritical fluid chromatography (SFC) is nowadays almost exclusively performed using compressed CO₂ as main component of the mobile phase [1,2]. Depending on the conditions (temperature and backpressure) and the amount of mobile phase modifier added to the CO₂ mobile phase (most commonly short chain alcohols such as methanol or ethanol), the actual fluid state under which the separation is performed is often not in truly supercritical conditions, but rather in the liquid or subcritical state [3,4]. Nevertheless, SFC is in practice used as a general name for all separations using CO₂ as the main component of the mobile phase [1,3]. The advantage of using sub- or supercritical CO₂ based mobile phases in terms of separation speed and efficiency becomes immediately clear from the equation describing the so-called Knox-Saleem (KS) limit, i.e. the maximum kinetic performance obtained when particle size and column length can freely be chosen, as [5]:

$$t_R = (1 + k) \cdot \frac{\eta \cdot \phi_0 \cdot h_{min}^2}{\Delta P_{max}} \cdot N^2 = (1 + k) \cdot \frac{\eta \cdot H_{min}^2}{\Delta P_{max} \cdot K_{V0}} \cdot N^2 \quad (1)$$

where η is the mobile phase viscosity, ϕ_0 the column flow resistance, K_{V0} the t_0 -based column permeability ($K_{V0} = d_p^2 / \phi_0$) and ΔP_{max} the maximum operating pressure or pressure drop over the column. As is clear from Eq. (1), the minimum analysis time t_R (or column void time t_0 for $k=0$) to reach a given efficiency N is proportional to the mobile phase viscosity and the maximum efficiency N for a given analysis time is proportional to $1/\sqrt{\eta}$. Comparing the viscosity of typical LC mobile phases at 30°C, such as water ($8.0 \cdot 10^{-4}$ Pa·s), methanol ($5.1 \cdot 10^{-4}$ Pa·s) and acetonitrile ($3.3 \cdot 10^{-4}$ Pa·s) and that of CO₂ at a pressure of 150 bar ($8.0 \cdot 10^{-5}$ Pa·s at 30°C and $5.7 \cdot 10^{-5}$ Pa·s at 50°C), indeed a decreases in analysis time around a factor of 10 can be expected and an improvement in efficiency of around 3. There are however several additional aspects to consider when evaluating Eq. (1). First of all, the above mentioned viscosities are only a first indication of the true viscosity of the mobile phases used, both for LC and SFC. Indeed, mixtures of MeOH and ACN with water have a higher viscosity than that of the pure organic solvents solvents [6]. This is however also the case in SFC as in almost all practical applications a significant amount of organic modifier is required [7], increasing the mobile phase viscosity. Indeed, in recent work, gradients spanning the entire range of pure CO₂ to pure modifier to separate compounds with a wide range of polarities have recently been implemented [8-11]. In addition, where commercial ultra-high performance LC instruments have maximum operating pressures in the range of 1200 to 1500 bar [12], a much more limited pressure range around 400 to 660 bar is available in SFC instrumentation [1,13,14]. For SFC, the need to apply a backpressure to maintain the mobile phase in the liquid or supercritical state also limits the available pressure drop over the column. As this backpressure is typically around 100-150 bar, only 250-550 bar pressure drop is available in a SFC instrument [9,13,14]. With the introduction of both smaller particle columns for use in SFC and the tendency to employ mobile phases with a significant fraction

of modifier, the need for higher operation pressure in SFC instrumentation is becoming more and more relevant. The final aspect is related to the column and system performance of SFC instrumentation. Whereas there is no fundamental reason that not the same minimum plate height can be achieved in SFC as in LC, most reports using narrower bore columns (2.1-3mm ID) show a much lower performance in SFC than when using modern UHPLC instrumentation. Although the measurement of performance data (such as van Deemter curves and kinetic plots) is more complicated and ambiguous in SFC than in LC due to the effect of pressure on separation parameters (retention, viscosity, density, diffusion coefficient...) [15-17], it is in most cases found that the main reason for this subpar performance is due to higher extra-column dispersion in SFC and due the injection solvent effects [13,14,18-20]. Indeed, where in LC the sample can often be dissolved in a mobile phase with equal or weaker elution strength as that at the start of the separation, this is impossible in SFC as here the mobile phase consist a compressed gas. Only if these limitations and difficulties can be resolved, the full advantage and possibilities of SFC separations for highly efficient and fast separations can be reached. It is important to note that Eq. (1) is only an approximation when using a compressible mobile phase such as is the case in SFC. The effect of pressure on the mobile phase density also causes retention gradients along the column, in addition to variations of the diffusion coefficients along its lengths due to variations in viscosity (see also Section 2).

As has become clear over the last decade, multi-dimensional separation techniques are a straightforward strategy to further increase separation resolution of complex samples [21]. The high orthogonality of SFC with many other separation techniques makes it an ideal technique to include in these systems, especially to implement e.g. a chiral separation step, although SFC faces significant challenges with regards to mobile phase compatibility between the two dimensions [22]. The possibility to perform very fast separation in SFC however makes it ideal for a second dimension in comprehensive 2D separation. In this work, the focus will however be on one dimensional separations. For the interested reader, two recent review papers provide an extensive overview of multi-dimensional techniques using SFC [23,24].

2. Limits of separation performance in SFC

As mentioned in the introduction, it is not straightforward to describe and predict separation performance in SFC due to the effects of pressure on separation parameters and performance [15-17]. However, in a first approximation, it can be assumed that same minimum plate height H_{min} can be obtained in SFC as in LC and that in reduced parameters ($h = H/d_p$ and $v = u \cdot d_p/D_{mol}$) the plate heights curves are similar. This allows to calculate and compare the kinetic performance limits in both LC and SFC, as detailed in earlier publications [25]. For more details on the construction and theoretical background of these plots, the reader is referred to literature [5,16,25,26].

In Fig. 1a a comparison is made between the limits of separation power in ultra-high pressure LC (UHPLC) at a maximum column pressure drop of 1500 bar and in SFC at 550 bar,

when using superficially porous particles. Note that this plot assumes that the entire pressure drop is available for the column (no extra-column pressure drop) and there is no significant contribution from extra-column dispersion. The dashed lines represent the KS-limit (see Eq. (1)) and the full line curves represent three typical particle sizes used in LC and SFC. It was assumed that the mobile phase in SFC ($\eta = 1 \cdot 10^{-4}$ Pa·s) is 10x less viscous than in LC ($\eta = 1 \cdot 10^{-3}$ Pa·s) and the diffusion (D_{mol}) 10x faster, and corresponding small molecule diffusion coefficients were chosen ($D_{\text{mol}} = 5 \cdot 10^{-10}$ m²/s in LC and $5 \cdot 10^{-9}$ m²/s in SFC). The clear advantage in separation performance of SFC over UHPLC, i.e. both a reduction in analysis time and an increase in efficiency, can be observed. The gain is however not as pronounced as would be expected based on the viscosity difference alone as the available maximum pressure drop in SFC is more limited with maximum commercially available instrument pressures around 600-660 bar and the requirement to maintain a backpressure of minimum around 100-120 bar. When a lower maximum instrument pressure is available (~400bar) and a higher backpressure is desired (~150bar), this further reduces to around 250 bar system pressure. This is represented in Fig. 1a by the shaded area representing the KS-limits between 250 and 550 bar, which approaches the UHPLC performance on the lower end of the pressure range. In addition, the estimated viscosity of the SFC mobile phase is only valid for relative low fraction of modifier in the mobile phase. Indeed for mobile phase gradients running up to pure modifier (e.g. methanol), viscosities close to that observed in LC are obtained, which limits the maximum flow rate that can be employed (see also Section 3.1). In fact, a pure methanol mobile phase at the end of the gradient in a unified chromatography separation (see Section 3.1) is around 50% more viscous than pure acetonitrile at the end of a RPLC gradient. This illustrates that, in order to access the full potential of SFC, instruments with the same pressure limits as available for LC should be developed, especially for applications that employ large modifier gradients. It was previously shown there are no fundamental limitations to perform analytical scale SFC separations in a pressure range up to 1050 bar [27], although the higher pressures affect the mobile phase viscosity and density and therefore also the plate height curves [7,17,27].

Another interesting observation that can be made from Fig. 1a is that in SFC the currently available sub-2 μ m particles are ideally suited for separations in the efficiency range around 5,000 to 50,000 theoretical plates, as the kinetic performance limit of the 1.5 μ m particles is close the KS-limit. For LC at 1500bar however, there is a significant deviation from this limit, indicating that in fact the currently available particles are sub-optimal for use in LC when a 1500 bar pressure limit is available. This observation is not surprising as the optimal particle size is proportional to $(\eta \cdot N / \Delta P)^{0.5}$ or $(\eta \cdot t_0 / \Delta P)^{0.25}$ [5]. It can also be understood from the fact that the diffusion and mass transfer is much faster in SFC than LC, allowing the use of larger particles with a longer diffusion distance.

Fig. 1b show the same data as Fig. 1a, limited to the case of SFC for sake of clarity, but now presents the corresponding column lengths to obtain the $t_{R,N}$ values show in Fig. 1a. Two observations can be made from these plots. First, to obtain very high efficiencies ($N \sim 100,000$), coupled columns packed with larger particles (2.5-3 μ m range) are needed with column length in the range of 50 tot 100cm. For fast separations requiring efficiencies in the range of $N = 10,000$ -30,000 column lengths of 3-10cm with small particles (sub-2 μ m) are the

best choice. When using such short, high efficiency columns, the contribution from extra-column dispersion become a major contributing factor to the total band broadening, strongly decreasing the overall separation resolution obtained in the column [28]. The relative contribution from these effects can be reduced by the use of large ID columns. However, as these fast separations are also achieved at high velocities, this comes at the cost of high flow rates, which can surpass the flow rate limitations of the instruments and strongly increase the solvent consumption. In addition, these high flow rates increase the extra-column pressure drop. It should also be noted that in some SFC instrumentation, the maximum flow rates decreases with increasing operating pressure, or vice-versa, the maximum operating pressure decreases when working at higher flow rates.

Using the methods described in earlier work in this journal [26], the effects of extra-column pressure and dispersion (see details in Figure caption) are illustrated in Fig. 2 for different column ID's. Note that it was assumed the flow remains laminar in all conditions, which will probably not be the case for high flow rates when using larger column IDs, so here the actual achievable performance can be overestimated. In addition, the extra-column band broadening is considered for a weakly retained component with a retention factor of 3 which are more affected by extra-column dispersion. Fig. 2 represents the same conditions as Fig. 1, but is limited to the KS-limit curves. Whereas the black dashed line presents the same case as the KS-limit for SFC in Fig. 1a, the full line curves illustrate the KS-limits (optimal t_R vs. N with optimized L and d_p) but taking the effects of extra-column dispersion and pressure drop into account. As expected, the narrower ID columns suffer more from the extra-column dispersion due to their lower column volume. In addition, it is clear that the largest deviation from the column KS-limit occurs in the lower efficiency range as this corresponds to the shortest column lengths (and thus lowest volumes) as shown in Fig. 1b. For the conditions where long column and larger particles sizes are more suited (top right), the effects of extra-column contributions become negligible. It should be noted that this theoretical calculation was performed assuming isocratic elution for a compound with retention factor $k=3$. In isocratic elution, early eluting compounds are more strongly affected by extra-column dispersion whereas late eluting compounds are almost not affected. On the other, in gradient elution, most compounds have more similar retention factors at point of elution ($k=1-3$ or lower) [28]. The pre-column dispersion is however less detrimental in gradient elution due to the on-column focusing. As a result, more or less the same behavior, at least qualitatively, will be observed in gradient elution, depending the magnitude of the post-column dispersion.

The theoretical considerations made in this section and the practical limitations of current generation SFC instrumentation have been observed in many research papers in the last decade. The research into ultra-fast separations in LC and SFC even inspired Gasparinni and co-workers to the subtitle of "The race to the shortest chromatogram" [29]. Many works have already reviewed the separation performance and speed of SFC (and LC) over the past years in a wide range of application areas [1,2,4,29-32]. Therefore the literature overview the following sections mainly focusses on research publications of the last three years (2018-2021).

3. Effect of mobile phase composition and separation conditions on efficiency

3.1 Large modifier content gradients

Over the last years, the application of gradient SFC for analysis of both very polar and apolar molecules has been investigated by several research groups [8-11,33-36]. In these analyses, the mobile phase start from (almost) pure CO₂ and ends with pure modifier (often pure MeOH), which also allows the analysis of larger (bio)molecules. Sometimes two distinct strategies are discerned here, either so-called enhanced fluidity liquid chromatography gradients (EFLC) or unified chromatography gradients (UC) [10,37,38]. For EFLC operation, the fraction of CO₂ is strongly limited (max. 30-40%) to allow a higher percentage of water (which is poorly miscible with CO₂) in the mobile phase [37-39]. For UC, the gradients span the entire range of CO₂ fractions, from (almost) pure CO₂ up to almost pure modifier. Recent review papers by Losacca et al. provide an overview of the applicability of SFC for polar compounds [37,40].

As discussed in Section 2, the use of a high fraction of organic modifier at the end of the gradient however affects the kinetic performance limits, as the maximum mobile phase viscosity determines the maximum pressure drop and thus the maximum flow rate that can be set or column length that can be used [9,10,41]. The problem can be alleviated by applying a concomitant composition and flow rate gradient, where the latter decreases during the run to compensate for the higher viscosity [42]. The flow rate gradient can be programmed such that an almost constant pressure is achieved during the run [43-45] or at least that it never exceeds the pressure limitation of the instrument. This requires some trial-and-error as the adsorption of mobile phase components on the stationary phase can affect the pressure profile [42]. Besides the obvious advantage in separation speed, this approach also allows to improve separation efficiency during the gradient run. Indeed, due to the change in viscosity during the gradient run, also the diffusion coefficient of the analytes strongly varies [43,44]. At the start, with a high fraction of CO₂, the solutes have a higher diffusion coefficient and thus require a higher flow rate to operate at the minimum of the van Deemter curve [9,46,47]. Near the end, the much lower diffusivity in the almost pure modifier requires lower flow rates. By tuning the flow rate program in such a way that the pressure drop remains almost constant, and assuming in a first approximation that D_{mol} is inversely proportional to the viscosity, one in fact can remain on the same location in the reduced plate height curve [43,44]. The inverse flow rate gradient thus avoids having to choose an intermediate flow rate to make a compromise in the separation efficiency of early and late eluting compounds [9,11]. The effect of composition on the optimal velocity was illustrated by Desfontaine et al. for a series of compounds with the same retention factor ($k=5$), as shown in Fig. 3 [9]. As can clearly be seen, the optimum velocity drops from 7-8 mm/s at 2% MeOH to around 2 mm/s (or 0.3 mL/min on a 3 mm ID column) for 80% of co-solvent.

Alternatively, one could consider a backpressure gradient where the backpressure is decreased near the end of the gradient to increase the available pressure drop for the

column [8]. For high fractions of CO₂ a higher backpressure (~150 bar) can be advantageous to avoid the high compressibility region around the critical point where mobile phase properties can strongly vary with small changes in operating parameters. Near the end of gradient, where more liquid like conditions are obtained, this is less relevant and lower backpressures can be applied. However, the available range to reduce the backpressure is rather limited (50-70 bar), although this is not negligible for SFC instruments with a maximum pressure rating around 400 bar [11]. Combined gradients of backpressure and flow rate were successfully applied by West and co-workers for the analysis of flavonoids and of free amino acids in food supplements [11,42]. It was also suggested that temperature gradients could be applied to decrease viscosity during the gradient [11], although this is not as flexible, accurate and fast with the currently available instrumentation and column hardware [48], unless in chip or capillary column systems [49]. It should also be noted that pressure, temperature or flow rate gradients should already be implemented during method development as otherwise the change in average pressure and temperature can affect retention and selectivity.

3.2 Effect of water in the mobile phase

With regards to mobile phase composition and additives, recent studies have illustrated how small amounts of water in the mobile phase can provide significant improvements in separation resolution in (a)chiral SFC [11,50-52], in addition to improving retention time repeatability due to the absence of silyl-ether formation. Although this was already illustrated in several earlier studies, the exact role of the water and the mechanisms were and are poorly understood [53-55]. As a rule of thumb, Khvalbota et al. found for a certain stationary phase that if the retention factor of the solute is larger than that of the water system peak, then the presence of water in the mobile phase will lead to improvements in efficiency [50]. This however did not hold for other investigated phases. In general, if there was a gain in efficiency, this was often most pronounced for the most retained analytes. Roy et al. observed up to an 8-fold increase in efficiency for chiral separations [52], although the addition of water always came with a decrease in retention and also affects selectivity [50,52]. The largest efficiency gains were observed for hydrophilic stationary phases and it was found that the addition of water could strongly reduce peak tailing [52]. This was recently confirmed by Firooz et al., showing a reduction in analysis time with increasing water content, but with a concomitant improvement in efficiency and peak symmetry for the separation of basic compounds on a benzoic acid functionalized cyclofructan-6 stationary phase [56]. An example chromatogram illustrating the effect of the addition of water on peak shape and performance is given in Fig. 4. In addition, using water rich modifier containing salts allows to further extent to use of SFC in the bioanalytical space [51]. Govender et al. showed how the use of water rich modifiers allowed to eliminate the need for acetonitrile for the SFC purification of insulin, while obtaining an average recovery of 84% [57]. In another study, the positive effect of the addition of water was used to replace methanol by azeotropic ethanol as co-solvent [58]. This solvent is less expensive and easy to recycle as it distills off at constant composition and contains ~4.6% water (often referred to as '190 proof'). It was found that azeotropic ethanol produced better efficiency and decreased retention times compared to pure methanol and ethanol. Although it was not

shown that ethanol/water is superior to methanol/water modifiers, as the comparison was only done relative to pure methanol, the use of azeotropic ethanol allows to make SFC an even more environmentally friendly separation technique and to replace methanol, which is toxic for humans, by a non-toxic biomass derived solvent.

3.3 Effect of temperature

Using elevated operating temperature is a well-known strategy in LC to increase separation speed by the decrease in mobile phase viscosity, but it is much less commonly used in SFC. Losacco et al. investigated the use of unconventional temperatures (from -5°C to 80°C) in a wide range of CO₂/MeOH concentrations (2 to 100% modifier) [13]. Whereas at low modifier concentrations the use of low temperatures did not translate in poor performance, the use of higher temperatures shifted the optimal temperature to such high flow rates that they were outside the range of the instrument for the employed 3.0 x 50mm 1.7µm particle column (see Fig. 5a). On the side of the high modifier concentrations (Fig. 5b) the use of elevated temperatures shows the same advantages as in UHPLC, which is not surprising as the mobile phase is here in a liquid like state. For intermediate concentrations, an operating temperature around 40°C was found the best choice from a kinetic performance point of view [13]. Looking at the corresponding pressure drop curves at high and low temperature (Figs. 5c and 5d respectively), the severe limitations of using low temperatures in combination with higher modifier content are clear as only a limited column pressure drop is available of around 250-300 bar. This again illustrates the limitations of current SFC instruments, where both limited maximum pressure and flow rate hinder the full use of the possibilities of SFC. With regards to retention, this study confirmed earlier reports that for low fractions of modifier, retention in fact increases with increasing temperature, due to the strong decrease in mobile phase density. At high modifier concentration, the traditional van 't Hoff behavior was observed, i.e. decreasing retention with increasing temperature. For intermediate modifier fractions, U-shaped van 't Hoff plot were found, as previously reported in chiral separations [59].

4. Innovations and trends in column technology

The advantages of the application of sub-2µm and superficially porous particles in SFC have been known for many years and were already reviewed by several authors [2,4,30,60-62]. In the past years however, many new stationary phases have been introduced or investigated (particles sizes, morphologies, chemistries...), especially for chiral analyses.

4.1 Superficially porous particles

As only a limited number of chiral stationary phases bonded to superficially porous particles (SPP) were commercially available prior to 2018 [2,63,64], a significant amount of research has been performed over the last years with either novel commercially available or in-house developed chiral SPP columns. For example, Barhate et al. successfully applied chiral SPP stationary phases for the enantiopurity analysis of verubecestat and its intermediates. Folprechtová et al. used 2.7µm chiral superficially porous particle stationary phases for the

separations of enantiomers of important biologically active compounds such as phytoalexins, substituted tryptophans and ketamine derivatives [65]. The same research groups also investigated vancomycin-based chiral stationary phases on the same support for the analysis of novel psychoactive substances, including pyrovalerones, benzofurans, phenidines and phenidates [66].

Roy and Armstrong compared the performance of 5 μ m fully porous particles with 2.7 μ m superficially porous ones for chiral analysis [63]. Although higher optimal flow rates F_{opt} (between +25% and +66% depending on the solute) and lower minimum plate height H_{min} (from 18.6 and 13.6 μ m for the 5 μ m fully porous to 12.5 and 9.2 μ m for the 2.7 μ m superficially porous) were obtained, these gains are lower than expected. Based on the particle size alone, both an increase in F_{opt} and a decrease in H_{min} by factor of 1.85 should be found and an even larger improvement would be expected due the use of the superficially porous particles. Besides extra-column dispersion effects, this lack of improvement in separation performance can be related to slow adsorption-desorption kinetics, as also observed for chiral separations in LC [62,67,68], which dominate the band broadening behavior of the columns. In addition, the smaller particle column possibly had a lower packing quality (higher A-term), yielding a higher h_{min} . Nevertheless, a significant improvement in separation performance at high flow rates was found for the 2.7 μ m particles compared to the 5 μ m ones. It should also be noted that the superficially porous particles typically yield lower retention factors than their fully porous counterparts due to a decreased amount of chiral selector. Using shorter (5cm) columns operated at very high flow rates (14mL/min), Roy and Armstrong were able to baseline separate several enantiomers in less than 30s [63]. Firooz et al. investigated two new functionalized cyclofructan columns (sulfonated cyclofructan-6 and benzoic acid functionalized cyclofructan-6) as polar stationary phases for achiral analysis, by modification of 2.7 μ m superficially porous particles using improved synthetic methodologies. [56] Efficiencies as high as 200,000 plates/m were obtained, yielding a reduced plate height of 1.8 in 4.6mm x 100mm columns.

The use of superficially porous particles not only allows very fast separations, but also very high efficiency separations if several columns are coupled in series. Lesselier et al. for example used a total length of 75 cm (5 x 150mm, 4.6mm ID) of columns packed with 2.6 μ m superficially porous particles for the analysis and quantification of triglycerides in SFC. [69]. This is in agreement with the observations made in Fig. 1b, where the optimal column lengths for these particle sizes was found to be in the 50 to 100cm range.

4.2 Fully porous particles

Few Sub-2 μ m chiral stationary phases were available up to 2017 and as a result only a few older reports existed of their use in SFC literature [46,47]. For example, in the years 2016-2018, research papers on achiral analytical-scale applications were majorly conducted on sub-2- μ m stationary phases, whereas chiral separations were still essentially conducted on larger particle sizes (2.5, 3, and 5 μ m). [2]

Ismail et al. were able to obtain efficiencies of 300-290,000 plates/m for retention factors of 1 and 2.5 on a 4.6mm ID column packed with 1.8 μ m Whelk-01 particles using a system with

minimized extra-column dispersion (see also Section 5) [70]. Recently He et al. used sub-2 μ m particles (1.6 μ m) for fast atropisomeric separation of a drug candidate, reducing analysis time 2.5x compared to a traditional 3 μ m stationary phase [71]. However, when comparing the van Deemter curves, little difference was observed between the 1.6 and 3 μ m particle column. Since the 1.6 μ m particle column had an inner diameter of 3.0mm and the 3 μ m particle column 4.6mm (both 10cm long), this was attributed to the much larger relative contribution from the extra-column dispersion on the smaller volume column. The authors also noted an increase in baseline noise due to pump pressure ripple at low flow rates (below 1.3mL/min), which could partially be alleviated by increasing the backpressure from 103 to 166bar. This however reduced the available pressure drop for the column and thus limited the maximum allowable flow rate. Kozlov et al. used intermediate sized fully porous particles (2.5 μ m) with a polysaccharide based stationary phases for the fast separations of 27 indole phytoalexins. [72] As is shown in Fig. 6, short columns (2cm) packed with 1.8 μ m particles allow very fast (<8s) achiral separations of 7 solutes with baseline resolution [18]. Terry Berger was able to obtain plate heights as low as 1.65 at a flow rate of 2.5mL/min on the same column with a system and column pressure drop of only 250 bar (backpressure at 100 bar) [73].

4.3 Chip and capillary-based SFC

Heiland et al. presented the first example of a microchip-based SFC system with packed chips and two-photon-excited-fluorescence detection [74]. The use of chips allows very efficient T-control, but it is challenging to obtain very low flow rates, control the backpressure and perform low volume injections. An elaborate set-up was developed that allowed to perform automated injections in a time span of only 9s. At linear velocities as high as 20 mm/s, the baseline separation of two enantiomers of Pirkle's alcohol was achieved in 12s with an efficiency of 9,500 plates/m when using 5 μ m particles. High reproducibility as well as excellent peak shapes were obtained. At lower velocities (~10.5 mm/s), efficiencies of 17,500-27,500 plates/m were obtained with 3 μ m particles for the separation of PAHs and 20,000 plates/m for napropamide enantiomers. The relative high reduced plate heights (~15-25) were explained by the very small column volume (100nL) and the comparatively large injection volume. Further development of this technique are thus required to optimize instrumentation and coupling to more universal detection techniques such as MS.

The low viscosity of the mobile phases used in traditional SFC, i.e. with a limited fraction of co-solvent, in combination with high flow rates results in a more common transition from laminar to turbulent flow in the connection capillaries than in LC [75,76] (see also Section 5.1). When considering open-tubular chromatographic systems, this transition can have advantages as the laminar parabolic flow profile in pressure driven flow is replaced by a more plug like flow profile, as only in a relatively thin boundary layer near the wall the velocity is different from the uniform bulk velocity. In addition, the faster radial dispersion due to the turbulent vortices across the diameter of the tube additionally reduces the mobile phase mass transfer resistance which is the dominant dispersion contribution in open-tubular systems at high velocity. This allows the use of larger ID capillaries than are

typically optimal for use in open-tubular LC and SFC systems (2.5 μ m or lower) [25]. Gritti and Fogwill developed theoretical models and experimentally verified the applicability of high-resolution turbulent flow chromatography [77-80]. When using pure CO₂ as mobile phase and a coated open tubular column, it was found that improvement in column performance from a laminar to a turbulent flow regime decreased with increasing retention factor in the range of $k=0$ -1 [80]. It was found that the mass transfer in turbulent flow was still controlled and limited by the slow sample transport across the viscous sublayer near the column wall, which still spans around 30% of the tube's cross sections. As a result, the benefits remain limited to small retention factors ($k<0.2$). Using a 20m long, 180 μ m ID capillary with 0.2 μ m film, ultra-fast analysis (<10s) of corone ($k\sim 0.1$) and its impurities was achieved, with a plate count of 33,000 at a Reynolds number around 5000. It therefore seems that, given the limited range of k in which these conditions are beneficial, the broad applicability of turbulent open tubular SFC is rather questionable.

5. Instrumentation and extra-column dispersion

The limitations of the new generation of SFC instrumentation with regards to extra-column band broadening and the need for modifications of the commercial instrumentation were pointed out several years ago [19,20,81,82]. With the introduction of novel (chiral) stationary phases and the pursuit of ultra-fast and high efficiency separations, these effects remain important to achieve the full performance potential of these highly efficient columns and continues to be investigated.

5.1 Optimization of extra-column dispersion

Ismail et al. modified a standard Waters UPC² instrument to a low dispersion equipment to by replacing the standard autosampler by an external valve with a 200nL loop, reducing the estimated [20] original 85 μ L² extra-column peak variance down to 29 μ L² [70]. By changing the standard 8 μ L detector cell to a 3 μ L one, this was further reduced to $\sigma_{V,EC}^2=15\mu\text{L}^2$ (see Entry-1 vs. 2 in Fig. 7). This confirms earlier reports that new low volume UV detector cells in SFC are essential to obtain the same low dispersion as currently available in UHPLC systems. Unfortunately, this can currently only be done using commercially available detector cells when these are used significantly above their maximum pressure rating [19]. By replacing the standard column oven with an external one and halving the length of the connecting tubing (from 120 to 60cm in total), a further decrease to $\sigma_{V,EC}^2=3.3\mu\text{L}^2$ was obtained with 180 μ m tubing (Entry-2 vs. 3 in Fig. 7). Further decreasing the tubing ID to 130 μ m or 100 μ m had limited effect ($\sigma_{V,EC}^2=2.2\mu\text{L}^2$ for both), probably due to the dominant contribution of the relative large UV flow cell [19,70]. The performance improvement of the low dispersion system was evident, especially for narrower ID columns (3.0mm) and weakly retained compounds showing an increase of almost 90% in efficiency compared to the standard instrument with only the external autosampler. The use of narrow ID capillaries can however induce turbulence, depending on tubing roughness, that can significantly increase extra-column pressure drop [17,18,47,73,75,76]. As a result, the use of narrow ID capillaries has a limited impact on $\sigma_{V,EC}^2$ if the other instrumental aspects are not optimized, but can result in

severe drawbacks. For example, Berger found that when using 75 μ m ID capillaries, up to 50% of the total system pressure drop was due to the connection tubing, whereas this was less than 10% when using 120 or 170 μ m tubing [17]. The (onset) of the turbulent flow regime, causing increased radial mixing in the cross section of the capillaries, could however in part explain the decreasing trend in $\sigma_{V,EC}^2$ with flow rate which is sometimes observed (see Fig. 7) [70].

Berger et al. modified an Agilent SFC system by using a low dispersion UV-cell (2 μ L vs. the standard 13 μ L), heat exchanger (125 μ m) and needle seat capillary (75 μ m). In addition, he replaced the standard 170 μ m tubing by shorter 120 μ m capillaries [18]. Since the instrument detector has an internal T control that reduces the mismatch between eluent and flow cell, the need for a post-column heat exchanger is eliminated, further reducing extra-column dispersion. With this system, having only an estimated 5 μ L² extra-column variance, reduced plate heights as low as 2.2 were obtained on a 3x20mm column packed with 1.8 μ m particles at 2.5mL/min and 7.5% methanol. Using higher flow rates and modified concentrations (5mL/min, 15% MeOH), 7 compounds from 4 different solute families were baseline separated in less than 8s as shown in Fig. 6. The authors noted that very high speed separations (~10s) in SFC are currently limited to the isocratic mode due to the very high gradient dwell volume in most systems, e.g. around 600 μ L, which yields gradient delays around 7.2s even at 5mL/min. For some peaks in the ultra-fast chromatogram, UV detector filters settings of 120 Hz and <16ms response time was required to avoid detection related peak broadening.

The limited advantage observed by Ismail et al. [70] when using narrower ID tubing of tubing was also observed by Berger when using 75 μ m ID capillaries. The author was however recently able to obtain reduced plate height values below 2 on a 2.1x100mm column with 1.8 μ m fully porous particles [17]. The van Deemter curve showed an unusual U-shaped profile, which was most pronounced for the narrow ID tubing, which was linked to the increased pressure in the column and resulting lower D_{mol} due to the large extra-column pressure drop. Berger also observed that switching from stainless steel to PEEK tubing reduced the extra-column pressure drop by one third as the smoother inner wall reduces the friction factor as previously observed by De Pauw et al. [75]. In earlier work, Berger investigated the effect of backpressure on separation performance using a 4.6mm x 150mm column packed with 5 μ m particles. Increasing backpressure did not change the minimum observed plate height but shifted the optimum velocity to lower values for low fractions of modifier (5 volume% MeOH). For higher modifier fractions (40 volume%) no change in either plate height or optimum velocity was observed.

6.2 Sample solvent effects and injection method

The importance of the injection solvent on the separation performance was studied in detail by Desfontaine et al. [83] but still remains an important factor in the optimization of separations methods in SFC [84]. To circumvent the detrimental effect of large-volume injections, Sun et al. investigated the feasibility of performing multiple subsequent small volume injections instead [85]. This method showed signal enhancement compared to a single large volume injection if the initial retention of the analytes was large enough to lead

to concentration on the column head, which was achieved by starting their gradient in a 100% CO₂ mobile phase. The effects of column overloading, dispersion during the delay in between injections and the migration of the analyte band in between injection decreased the efficiency of the technique, especially for poorly and moderately retained compounds. The advantages of this technique are therefore dependent on the injected solutes and the stationary phase, but also on the employed gradient program.

An alternative injection method, the so-called feed injector, was recently introduced by Agilent Technologies on their SFC instrument. Whereas typically a loop is switched in-line with the mobile phase flow path to inject the sample, this feed injector adds the sample volume to the mobile phase flow, increasing the total flow rate for a short time [86]. This yields only a limited increase in pressure drop due to the compressible nature of the mobile phase in SFC. Additionally, the introduction of a higher viscosity plug in the flow path always causes a pressure spike. The fact that the sample is mixed with the mobile phase causes two phenomena that have an opposite effect on band broadening. Whereas the dilution of the sample inherently results in the injection of a larger sample volume, the concomitant mixing of the sample solvent with the mobile phase reduces the solvent mismatch and its associated band broadening effects [19,83]. Vanderlinden et al. investigated this injection method in detail and found that the optimal ratio F_{feed}/F of injection flow rate (F_{feed}) over mobile phase flow rate F is independent on the employed F [86]. This is not unexpected as a fixed F_{feed}/F results in the same dilution of sample plug and sample solvent. Surprisingly, the optimal F_{feed}/F -ratios for the investigate compounds and column (hormones and bare silica) were rather low, around 0.2-0.3, showing that a strong dilution of the sample solvent was advantageous even though this resulted in a strong increase of the volume of the injected sample plug. The overfeed solvent plug, required to fully inject the loaded sample volume, was found to have a detrimental effect on the peak width, as was also observed by Berger [18,86]. Switching from methanol to hexane as overfeed solvent resulted in a significant decrease in band broadening and an almost negligible effect of overfeed volume on peak width [86]. Alternatively, it was investigated if the sample itself could be used as overfeed solvent. This resulted in even narrower peaks than when using hexane as overfeed solvent, however this technique was not suitable for small volume injections (< 0.5-1 μ L) as it suffered from poorer reproducibility and precision [86].

6. Conclusions

The use of CO₂ as the main component of the mobile phase allows to achieve highly efficient and fast separations due to the significantly lower viscosity than typical LC mobile phases. However, as the application area of SFC is shifting towards larger and more polar molecules, mobile phases with viscosities close to those used in LC are being used, strongly reducing this kinetic performance benefit. These new trends thus require either an improvement in the instrumental capabilities (higher operating pressures) or the implementation of flow rate and backpressure gradients. As more liquid like conditions are common, the use of elevated temperatures (or even temperature gradients) is another interesting possibility. In addition, it has become clear that current generation SFC are not designed to be used with the current

generation of highly efficient columns packed with small superficially porous particles. When these columns are used in the traditional 4.6mm ID format, the required flow rates often exceed those of the instrumentation and result in excessive extra-column pressure in the fluidic path due to occurrence of turbulent flow. When narrower ID columns are used (2.1-3mm), the much smaller column volumes are no longer compatible with the much larger extra-column variance in SFC instrumentation compared to UHPLC. The pressure requirement for the UV flow cells however seems to limit the possibilities to further reduce and optimize their design. In addition, the compatibility of the injection solvent with the SFC mobile phase remains a challenge, both in one-dimensional chromatography and for the use of SFC in multidimensional setups.

540

Figure Captions

Figure 1: Kinetic performance limits for UHPLC ($\Delta P=1500$ bar) and SFC ($\Delta P=550$ bar) assuming $\eta = 1 \cdot 10^{-3}$ Pa·s and $D_{\text{mol}} = 5 \cdot 10^{-10}$ m²/s for LC and $\eta = 1 \cdot 10^{-4}$ Pa·s and $D_{\text{mol}} = 5 \cdot 10^{-9}$ m²/s for SFC. For both modes, $\phi_0 = 650$, $h = a + b/v + c \cdot v$ and $a = 0.8$, $b = 3$ and $c = 0.06$ with the particles sizes indicated on the figure. To calculate the retention time t_R , a retention factor of $k=9$ was assumed. The dashed lines represent the Knox-Saleem limits (see Eq. (1)) for both techniques. **(a)** Plot of analysis time vs. efficiency. The colored area represents the Knox-Saleem limit range for $\Delta P=250$ -550 bar in SFC; **(b)** Plot of corresponding columns lengths vs efficiency (SFC only).

Figure 2: Plot of the kinetic performance limits when using fully optimized flow rate, column length and particle size, i.e. the Knox and Saleem limit for SFC under the same conditions as Fig. 1. The dashed line represent the Knox-Saleem limits according to Eq. (1), without any extra-column contributions (dispersion and pressure drop) and the full lines with these effects for three different column ID's. Extra-column tubing: 50cm x 125 μ m (2x, pre- and post-column), extra-column variance due to injection = 2 μ L² and detector = 3 μ L². Retention time calculated for a last eluting compound of $k=9$, extra-column dispersion contribution calculated for $k=4$.

Figure 3: Van Deemter curves for different compounds with similar retention factor ($k \sim 5$) for different fractions of modifier (MeOH/water, 95/5 v%/v%) in the mobile phase at 40°C and 150 bar. Reprinted with permission from [9].

Figure 4: SFC chromatogram of 3,5-dinitrobenzoic acid on a FructoSheel-N column (2.7 μ m superficially porous particles, 4.6 x 100mm) with 90/10 CO₂/MeOH + 0.1% (v%/v%) TEA + 0.1% (v%/v%) TFA mobile phase with (top, red) and without (bottom, black) the addition of 5.7% (v/v) of water to the modifier phase. Note that the 0.57% (v%/v%) on the figure indicates the water fraction in the total mobile phase. Reprinted with permission from [50].

Figure 5: (a-b) van Deemter plots corrected for extra-column dispersion, obtained at five different co-solvent percentages and temperatures (see figure legend) **(a)** for butylparaben with MeOH/H₂O 95/5 v%v% as co-solvent and **(b)** for indoxyl sulphate with MeOH/H₂O 95/5 v%/v% + 10 mM of ammonium formate as co-solvent. For each analyte and condition the retention factor had a minimal value of at least 5; (c-d) Pressure plots recorded under isocratic conditions at different conditions (see figure legend) for temperatures of **(c)** 80°C and **(d)** -5 °C. Adapted and reprinted with permission from [13].

Figure 6: Fast, efficient separation of a 7 component mixture at 5mL/min, 15 v% MeOH in CO₂ at 40°C and 100 bar backpressure using a 3 x 20mm, 1.8 μ m RX-Sil. Pump pressure of 435 bar using a modified Agilent 1260 II SFC with a 120 Hz detector, an injection volume of 0.2 μ L, 1 μ L overfeed volume and 1000 μ L/min feed flow rate. Reprinted with permission from [18].

Figure 7: Extra-column variance contribution of the SFC instrument calculated using the method of moments for different configurations of a Waters UPC² instrument, with Entry-1 the system as-shipped but with the standard injector replaced by an external valve with a 0.2 μ L loop. Modification in Entries 2-5 as discussed in the text and specified in [70]. Reprinted with permission from [70].

References

- [1] C. West, Current trends in supercritical fluid chromatography, *Analytical and Bioanalytical Chemistry* 410 (2018) 6441–6457. <https://doi.org/10.1007/s00216-018-1267-4>
- [2] Lesellier E, West C. The many faces of packed column supercritical fluid chromatography - a critical review. *Journal of Chromatography A*. 1382 (2015) 2–46. <https://doi.org/10.1016/j.chroma.2014.12.083>.
- [3] Tarafder A. Metamorphosis of supercritical fluid chromatography to SFC: an overview. *TrAC Trends in Analytical Chemistry* 81 (2016) 3–10. <https://doi.org/10.1016/j.trac.2016.01.002>.
- [4] Nováková L, Grand-Guillaume Perrenoud A, Francois I, West C, Lesellier E, Guillarme D. Modern analytical supercritical fluid chromatography using columns packed with sub-2 μm particles: a tutorial. *Anal Chim Acta*. 824 (2014) 18-35. <https://doi.org/10.1016/j.aca.2014.03.034>
- [5] K. Broeckhoven, G. Desmet, Advances and Challenges in Extremely High-Pressure Liquid Chromatography in Current and Future Analytical Scale Column Formats, *Analytical Chemistry* 92 (2020) 554–560. <https://doi.org/10.1021/acs.analchem.9b04278>
- [6] J. Billen, K. Broeckhoven, A. Liekens, K. Choikhet, G. Rozing, G. Desmet, Influence of pressure and temperature on the physico-chemical properties of mobile phase mixtures commonly used in high-performance liquid chromatography, *Journal of Chromatography A* 1210 (2008) 30-44.
- [7] T.A. Berger, Effect of density on kinetic performance in supercritical fluid chromatography with methanol modified carbon dioxide, *Journal of Chromatography A* 1564 (2018) 188-198. <https://doi.org/10.1016/j.chroma.2018.06.021>
- [8] K. Taguchi, E. Fukusaki, T. Bamba, Simultaneous analysis for water- and fat-soluble vitamins by a novel single chromatography technique unifying supercritical fluid chromatography and liquid chromatography, *Journal of Chromatogr A* 1362 (2014) 270–277. <https://doi.org/10.1016/j.chroma.2014.08.003>.
- [9] V. Desfontaine, G.L. Losacco, Y. Gagnebin, J. Pezzatti, W.P. Farrell, V. González-Ruiz, S. Rudaz, J.-L. Veuthey, D. Guillarme, Applicability of supercritical fluid chromatography - mass spectrometry to metabolomics. I - optimization of separation conditions for the simultaneous analysis of hydrophilic and lipophilic substances, *J. Chromatogr., A* 1562 (2018) 96-107, <https://doi.org/10.1016/j.chroma.2018.05.055>.
- [10] A. Raimbault, M. Dorebska, C. West, A chiral unified chromatography–mass spectrometry method to analyze free amino acids, *Analytical and Bioanalytical Chemistry* 411 (2019) 4909–4917. <https://doi.org/10.1007/s00216-019-01783-5>.
- [11] A. Raimbault, A. Noireau, C. West, Analysis of free amino acids with unified chromatography-mass spectrometry-application to food supplements, *Journal of Chromatography A* 1616 (2020) 460772. <https://doi.org/10.1016/j.chroma.2019.460772>
- [12] J. De Vos, K. Broeckhoven, S. Eeltink, Advances in Ultrahigh-Pressure Liquid Chromatography Technology and System Design, *Analytical Chemistry* 88 (2016) 262–278. <https://doi.org/10.1021/acs.analchem.5b04381>

619 [13] G.L. Losacco, S.Fekete, J.-L. Veuthey, D.Guillarme, Investigating the use of unconventional
620 temperatures in supercritical fluid chromatography, *Analytica Chimica Acta* 1134 (2020) 84-95.
621 <https://doi.org/10.1016/j.aca.2020.07.076>

622 [14] S. Olesik, C. West, D. Guillarme, D. Mangelings, L. Novakova, Analytical challenges encountered
623 and the potential of supercritical fluid chromatography: A perspective of five experts, *Analytical*
624 *Science Advances* 2 (2021) 76–80. <https://doi.org/10.1002/ansa.202000151>

625 [15] D.P. Poe, *Supercritical Fluid Chromatography: Chapter 2 - Theory of Supercritical Fluid*
626 *Chromatography*, Ed. C. F. Poole, Elsevier (2017) 23-55. [http://dx.doi.org/10.1016/B978-0-12-](http://dx.doi.org/10.1016/B978-0-12-809207-1.00002-1)
627 [809207-1.00002-1](http://dx.doi.org/10.1016/B978-0-12-809207-1.00002-1)

628 [16] K. Broeckhoven, G. Desmet, Methods to determine the kinetic performance limit of
629 contemporary chromatographic techniques, *Journal of Separation Science* 44 (2020) 323-339
630 <https://doi.org/10.1002/jssc.202000779>.

631 [17] T.A. Berger, Diffusion and Dispersion in Tubes in Supercritical Fluid Chromatography Using Sub-2
632 μm Packings, *Chromatographia* 84 (2021) 167–177. <https://doi.org/10.1007/s10337-020-03996-8>

633 [18] T.A. Berger, High-Speed, High-Efficiency Achiral SFC on a $3 \times 20\text{-mm}$ Column Packed with $1.8\text{-}\mu\text{m}$
634 Particles Facilitated by a Low-Dispersion Chromatograph, *Chromatographia* 82 (2019) 537–542.
635 <https://doi.org/10.1007/s10337-018-3655-5>

636 [19] R. De Pauw, K. Shoykhet (Choikhet), G. Desmet, K. Broeckhoven, Understanding and diminishing
637 the extra-column band broadening effects in supercritical fluid chromatography, *Journal of*
638 *Chromatography A* 1403 (2015) 132-137. <https://doi.org/10.1016/j.chroma.2015.05.017>

639 [20] A. Grand-Guillaume Perrenoud, C. Hamman, M. Goel, J.-L. Veuthey, D. Guillarme, S. Fekete,
640 Maximizing kinetic performance in supercritical fluid chromatography using state-of-the-art
641 instruments, *Journal of Chromatography A* 1314 (2013) 288-297.
642 <https://doi.org/10.1016/j.chroma.2013.09.039>

643 [21] M. Edwards, H. Boswell, T. Górecki, *Comprehensive Multidimensional Chromatography*, *Current*
644 *Chromatography* 2 (2015) 80–109. <https://doi.org/10.2174/2213240602666150722232236>

645 [22] M. Sarrut, A. Corgier, G. Crétier, A. Le Masle, S. Dubant, S. Heinisch, Potential and limitations of
646 on-line comprehensive reversed phase liquid chromatography \times supercritical fluid chromatography for
647 the separation of neutral compounds: An approach to separate an aqueous extract of bio-oil, *Journal*
648 *of Chromatography A* 1402 (2015) 124-133. <https://doi.org/10.1016/j.chroma.2015.05.005>

649 [23] A.S. Kaplitz, M.E. Mostafa, S.A. Calvez, J.L. Edwards, J.P. Grinias, Two-dimensional separation
650 techniques using supercritical fluid chromatography, *Journal of Separation Science* 44 (2021) 426-
651 437. <https://doi.org/10.1002/jssc.202000823>

652 [24] M. Burlet-Parendel, K. Faure, Opportunities and challenges of liquid chromatography coupled to
653 supercritical fluid chromatography, *TrAC Trends in Analytical Chemistry* 144 (2021) 116422.
654 <https://doi.org/10.1016/j.trac.2021.116422>.

655 [25] S. Jespers, K. Broeckhoven, G. Desmet, Comparing the Separation Speed of Contemporary LC,
656 SFC, and GC, *LCGC Europe* 30 (2017) 284-291.

657 [26] K. Broeckhoven, G. Desmet, The future of UHPLC: Towards higher pressure and/or smaller
658 particles?, *TrAC Trends in Analytical Chemistry* 63 (2014) 65-75.
659 <https://doi.org/10.1016/j.trac.2014.06.022>

660 [27] R. De Pauw, K. Shoykhet (Choikhet), G. Desmet, K. Broeckhoven, Exploring the speed-resolution
661 limits of supercritical fluid chromatography at ultra-high pressures, *Journal of Chromatography A*
662 1374 (2014) 247-253. <https://doi.org/10.1016/j.chroma.2014.11.056>

663 [28] G. Desmet, K. Broeckhoven, Extra-column band broadening effects in contemporary liquid
664 chromatography: Causes and solutions, *TrAC Trends in Analytical Chemistry* 119 (2019) 115619.
665 <https://doi.org/10.1016/j.trac.2019.115619>

666 [29] A. Ciogli, O. H. Ismail, G. Mazzocanti, C. Villani, F. Gasparrini, Enantioselective ultra high
667 performance liquid and supercritical fluid chromatography: The race to the shortest chromatogram,
668 *Journal of Separation Science* 41 (2018) 1307–1318. <https://doi.org/10.1002/jssc.201701406>

669 [30] S. Felletti, O.H. Ismail, C. De Luca, V. Costa, F. Gasparrini, L. Pasti, N. Marchetti, A. Cavazzini, M.
670 Catani, Recent Achievements and Future Challenges in Supercritical Fluid Chromatography for the
671 Enantioselective Separation of Chiral Pharmaceuticals, *Chromatographia* 82 (2019) 65–75.
672 <https://doi.org/10.1007/s10337-018-3606-1>

673 [31] A. S. Kaplitz, G. A. Kresge, B. Selover, L. Horvat, E. G. Franklin, J. M. Godinho, K. M. Grinias, S. W.
674 Foster, J. J. Davis, J. P. Grinias, High-Throughput and Ultrafast Liquid Chromatography, *Analytical*
675 *Chemistry* 92 (2020) 67–84. <https://doi.org/10.1021/acs.analchem.9b04713>

676 [32] C. West, Recent trends in chiral supercritical fluid chromatography, *Trends in Analytical*
677 *Chemistry* 120 (2019) 115648. <https://doi.org/10.1016/j.trac.2019.115648>

678 [33] Y. Huang, T. Zhang, Y. Zhao, H. Zhou, G. Tang, M. Fillet, J. Crommen, Z. Jiang, Simultaneous
679 analysis of nucleobases, nucleosides and ginsenosides in ginseng extracts using supercritical fluid
680 chromatography coupled with single quadrupole mass spectrometry, *Spec. Issue Honor Retire. Prof*
681 *Carlo Bertucci*. 144 (2017) 213-219, <https://doi.org/10.1016/j.jpba.2017.03.059>.

682 [32] T. Lefebvre, A. Talbi, S. Atwi-Ghaddar, E. Destandau, E. Lesellier, Development of an analytical
683 method for chlorophyll pigments separation by reversed phase supercritical fluid chromatography, *J.*
684 *Chromatogr., A* 1612 (2020) 460643, <https://doi.org/10.1016/j.chroma.2019.460643>.

685 [33] G.L. Losacco, O. Ios, J. Pezzatti, V. Gonzalez-Ruiz, J. Boccard, S. Rudaz, J.-L. Veuthey, D. Guillarme,
686 Applicability of Supercritical fluid chromatography-Mass spectrometry to metabolomics. II-
687 Assessment of a comprehensive library of metabolites and evaluation of biological matrices, *J.*
688 *Chromatogr. A* (2020) 461021, <https://doi.org/10.1016/j.chroma.2020.461021>.

689 [36] B. van de Velde, D. Guillarme, I. Kohler, Supercritical fluid chromatography – Mass spectrometry
690 in metabolomics: Past, present, and future perspectives, *Journal of Chromatography B* 1161 (2020)
691 122444. <https://doi.org/10.1016/j.jchromb.2020.122444>

692 [37] G. L. Losacco, J.-L. Veuthey, D. Guillarme, Metamorphosis of supercritical fluid chromatography:
693 A viable tool for the analysis of polar compounds?, *TrAC Trends in Analytical Chemistry* 141 (2021)
694 116304. <https://doi.org/10.1016/j.trac.2021.116304>

695 [38] Y. Wang, S. V. Olesik, Enhanced-Fluidity Liquid Chromatography–Mass Spectrometry for Intact
696 Protein Separation and Characterization, *Analytical Chemistry* 91 (2019) 935–942.
697 <https://doi.org/10.1021/acs.analchem.8b03970>

698 [39] R. Bennett, S. V. Olesik, Enhanced fluidity liquid chromatography of inulin fructans using ternary
699 solvent strength and selectivity gradients, *Analytica Chimica Acta* 999 (2018) 161-168.
700 <https://doi.org/10.1016/j.aca.2017.10.036>

701 [40] G. L. Losacco, J.-L. Veuthey, D. Guillarme, Supercritical fluid chromatography – Mass
702 spectrometry: Recent evolution and current trends, *TrAC Trends in Analytical Chemistry* 118 (2019)
703 731-738. <https://doi.org/10.1016/j.trac.2019.07.005>

704 [41] D. Wolrab, P. Frühauf, C. Gerner, M. Kohout, W. Lindner, Consequences of transition from liquid
705 chromatography to supercritical fluid chromatography on the overall performance of a chiral
706 zwitterionic ion-exchanger, *Journal of Chromatography A* 1517 (2017) 165-175.
707 <https://doi.org/10.1016/j.chroma.2017.08.022>

708 [42] Chromatographic analysis of biomolecules with pressurized carbon dioxide mobile phases - A
709 review, J. Molineau, M. Hideux, C. West, *Journal of Pharmaceutical and Biomedical Analysis*, 193
710 (2021) 113736, <https://doi.org/10.1016/j.jpba.2020.113736>

711 [43] K. Broeckhoven, M. Verstraeten, K. Choikhet, M. Dittmann, K. Witt, G. Desmet, Kinetic
712 performance limits of constant pressure versus constant flow rate gradient elution separations. Part
713 I: Theory, *Journal of Chromatography A* 1218 (2011) 1153-1169.
714 <https://doi.org/10.1016/j.chroma.2010.12.086>

715 [44] M. Verstraeten, K. Broeckhoven, M. Dittmann, K. Choikhet, K. Witt, G. Desmet, Kinetic
716 performance limits of constant pressure versus constant flow rate gradient elution separations. Part
717 II: Experimental, *Journal of Chromatography A* 1218 (2011) 1170-1184.
718 <https://doi.org/10.1016/j.chroma.2010.12.087>

719 [45] R. De Pauw, G. Desmet, K. Broeckhoven, Theoretical evaluation of the advantages and
720 limitations of constant pressure versus constant flow rate gradient elution separation in supercritical
721 fluid chromatography, *Journal of Chromatography A* 1312 (2013) 134-142.
722 <https://doi.org/10.1016/j.chroma.2013.09.008>

723 [46] T. A. Berger, Kinetic performance of a 50 mm long 1.8 μ m chiral column in supercritical fluid
724 chromatography, *Journal of Chromatography A*, 1459 (2016) 136-144,
725 <http://dx.doi.org/10.1016/j.chroma.2016.07.012>

726 [47] T.A. Berger, Preliminary kinetic evaluation of an immobilized polysaccharide sub-2 μ m column
727 using a low dispersion supercritical fluid chromatograph, *Journal of Chromatography A*, 1510 (2017)
728 82-88. <http://dx.doi.org/10.1016/j.chroma.2017.06.021>

729 [48] M. Baert, Kristina Wicht, A. Moussa, G. Desmet, K. Broeckhoven, F. Lynen, Implementations of
730 temperature gradients in temperature-responsive liquid chromatography, *Journal of*
731 *Chromatography A* 1654 (2021) 462425. <https://doi.org/10.1016/j.chroma.2021.462425>

732 [49] J. J. Heiland, C. Lotter, V. Stein, L. Mauritz, D. Belder, Temperature Gradient Elution and
733 Superheated Eluents in Chip-HPLC, *Analytical Chemistry* 89 (2017) 3266-3271.
734 <https://doi.org/10.1021/acs.analchem.7b00142>

735 [50] L. Khvalbota, D. Roy, M. F. Wahab, S. K. Firooz, A. Machynáková, I. Spánik, D. W. Armstrong,
736 Enhancing supercritical fluid chromatographic efficiency: Predicting effects of small aqueous
737 additives, *Anal. Chim. Acta* 1120 (2020) 75-84. <https://doi.org/10.1016/j.aca.2020.04.065>

738 [51] J. Liu, A.A. Makarov, R. Bennett, I.A. Haidar Ahmad, J. DaSilva, M. Reibarkh, I. Mangion, B.F.
739 Mann, E.L. Regalado, Chaotropic effects in sub/supercritical fluid chromatography via ammonium
740 hydroxide in water-rich modifiers: enabling separation of peptides and highly polar pharmaceuticals
741 at the preparative scale, *Anal. Chem.* 91 (2019) 13907-13915.
742 <https://doi.org/10.1021/acs.analchem.9b03408>

743 [52] D. Roy, M.F. Wahab, T.A. Berger, D.W. Armstrong, Ramifications and insights on the role of
 744 water in chiral sub/supercritical fluid chromatography, *Anal. Chem.* 91 (2019) 14672-14680.
 745 <https://doi.org/10.1021/acs.analchem.9b03908>

746 [53] M. Ashraf-Khorassani, L.T. Taylor, Subcritical fluid chromatography of water soluble nucleobases
 747 on various polar stationary phases facilitated with alcohol-modified CO₂ and water as the polar
 748 additive, *J. Separ. Sci.* 33 (11) (2010) 1682-1691. <https://doi.org/10.1002/jssc.201000047>

749 [54] L.T. Taylor, Packed column supercritical fluid chromatography of hydrophilic analytes via water-
 750 rich modifiers, *J. Chromatogr. A* 1250 (2012) 196-204. <https://doi.org/10.1016/j.chroma.2012.02.037>

751 [55] J. Liu, E.L. Regalado, I. Mergelsberg, C.J. Welch, Extending the range of supercritical fluid
 752 chromatography by use of water-rich modifiers, *Org. Biomol. Chem.* 11 (2013) 4925-4929.
 753 <https://doi.org/10.1039/C3OB41121D>

754 [56] High efficiency functionalized hydrophilic cyclofructans as stationary phases in sub/supercritical
 755 fluid chromatography, S. K. Firooz, M. F. Wahab, J. Yu, D. W. Armstrong, *Journal of Chromatography*
 756 *A* 1645 (2021) 462129. <https://doi.org/10.1016/j.chroma.2021.462129>

757 [57] K. Govender, T. Naicker, S. Baijnath, A. A. Chuturgoon, N. S. Abdul, T. Docrat, H. G. Kruger, T.
 758 Govender, Sub/supercritical fluid chromatography employing water-rich modifier enables the
 759 purification of biosynthesized human insulin, *Journal of Chromatography B* 1155 (2020) 122126.
 760 <https://doi.org/10.1016/j.jchromb.2020.122126>

761 [58] D. Roy, M. F. Wahab, M. Talebi and D. W. Armstrong, Replacing methanol with azeotropic
 762 ethanol as the co-solvent for improved chiral separations with supercritical fluid chromatography
 763 (SFC), *Green Chemistry* 22 (2020) 1249-1257. <https://doi.org/10.1039/c9gc04207e>

764 [59] R.W. Stringham, J.A. Blackwell, "Entropically driven" chiral separations in supercritical fluid
 765 chromatography. Confirmation of isoelution temperature and reversal of elution order, *Anal. Chem.*
 766 68 (1996) 2179-2185. <https://doi.org/10.1021/ac960029e>.

767 [60] A. Grand-Guillaume Perrenoud, W.P. Farrell, C.M. Aurigemma, N.C. Aurigemma, S.Fekete, D.
 768 Guillarme, Evaluation of stationary phases packed with superficially porous particles for the analysis
 769 of pharmaceutical compounds using supercritical fluid chromatography, *Journal of Chromatography*
 770 *A* 1360 (2014) 275-287. <https://doi.org/10.1016/j.chroma.2014.07.078>

771 [61] A. Grand-Guillaume Perrenoud, J.-L. Veuthey, D. Guillarme, Comparison of ultra-high
 772 performance supercritical fluid chromatography and ultra-high performance liquid chromatography
 773 for the analysis of pharmaceutical compound, *Journal of Chromatography A* 1266 (2012) 158-16.
 774 <https://doi.org/10.1016/j.chroma.2012.10.005>

775 [62] O.H. Ismail, A. Ciogli, C. Villani, M. De Martino, M. Pierini, A. Cavazzini, D.S. Bell, F. Gasparri,
 776 Ultra-fast high-efficiency enantioseparations by means of a teicoplanin-based chiral stationary phase
 777 made on sub-2 μ m totally porous silica particles of narrow size distribution, *Journal of*
 778 *Chromatography A* 1427 (2016) 55-68. <https://doi.org/10.1016/j.chroma.2015.11.071>

779 [63] D. Roy, D. W. Armstrong, Fast super/subcritical fluid chromatographic enantioseparations on
 780 superficially porous particles bonded with broad selectivity chiral selectors relative to fully porous
 781 particles, *Journal of Chromatography A*, 1605 (2019) 360339.
 782 <https://doi.org/10.1016/j.chroma.2019.06.060>

783 [64] C.L. Barhate, D.A. Lopez, A.A. Makarov, X. Bub, W.J. Morris, A. Lekhal, R. Hartman, D.W.
784 Armstrong, E.L. Regalado, Macrocyclic glycopeptide chiral selectors bonded to core-shell particles
785 enables enantiopurity analysis of the entire verubecestatin synthetic route, *Journal of Chromatography*
786 *A*, 1539 (2018) 87–92. <https://doi.org/10.1016/j.chroma.2018.01.042>

787 [65] D. Folprechtová, O. Kozlov, D. W. Armstrong, M. G. Schmid, K. Kalíková, E. Tesarová,
788 Enantioselective potential of teicoplanin- and vancomycin-based superficially porous particles-
789 packed columns for supercritical fluid chromatography, *Journal of Chromatography A* 1612 (2020)
790 160687. <https://doi.org/10.1016/j.chroma.2019.460687>

791 [66] D. Folprechtová, K. Kalíková, Kian Kадkhodaei, C. Reiterer, D. W. Armstrong, E. Tesarová, M. G.
792 Schmid, Enantioseparation performance of superficially porous particle vancomycin-based chiral
793 stationary phases in supercritical fluid chromatography and high performance liquid
794 chromatography; applicability for psychoactive substances, *Journal of Chromatography A* 1637
795 (2021) 461846. <https://doi.org/10.1016/j.chroma.2020.461846>

796 [67] C. Geibel, K. Dittrich, U. Woiwode, M. Kohout, T. Zhang, W. Lindner, M. Lämmerhofer,
797 Evaluation of superficially porous particle based zwitterionic chiral ion exchangers against fully
798 porous particle benchmarks for enantioselective ultra-high performance liquid chromatography,
799 *Journal of Chromatography A* 1603 (2019) 130–140. <https://doi.org/10.1016/j.chroma.2019.06.026>

800 [68] Salome Pantsulaia, K. Targamadze, N. Khundadze, Qe. Kharashvili, A. Volonterio, M. Chitty, T.
801 Farkas, B. Chankvetadze, Potential and current limitations of superficially porous silica as a carrier for
802 polysaccharide-based chiral selectors in separation of enantiomers in high-performance liquid
803 chromatography, *Journal of Chromatography A* 1625 (2020) 461297.
804 <https://doi.org/10.1016/j.chroma.2020.461297>

805 [69] E. Lesellier, A. Latos, C. West, Ultra high efficiency/low pressure supercritical fluid
806 chromatography (UHE/LP-SFC) for triglyceride analysis: Identification, quantification, and
807 classification of vegetable oils, *Analytical Science Advances* 2 (2021) 33–42.
808 <https://doi.org/10.1002/ansa.202000156>

809 [70] O.H. Ismail, G.L. Losacco, G. Mazzocanti, A. Ciogli, C. Villani, M. Catani, L. Pasti, S. Anderson, A.
810 Cavazzini, F. Gasparrini, Unmatched Kinetic Performance in Enantioselective Supercritical Fluid
811 Chromatography by Combining Latest Generation Whelk-O1 Chiral Stationary Phases with a Low-
812 Dispersion in-House Modified Equipment, *Analytical Chemistry* 90 (2018) 10828–10836.
813 <https://doi.org/10.1021/acs.analchem.8b01907>

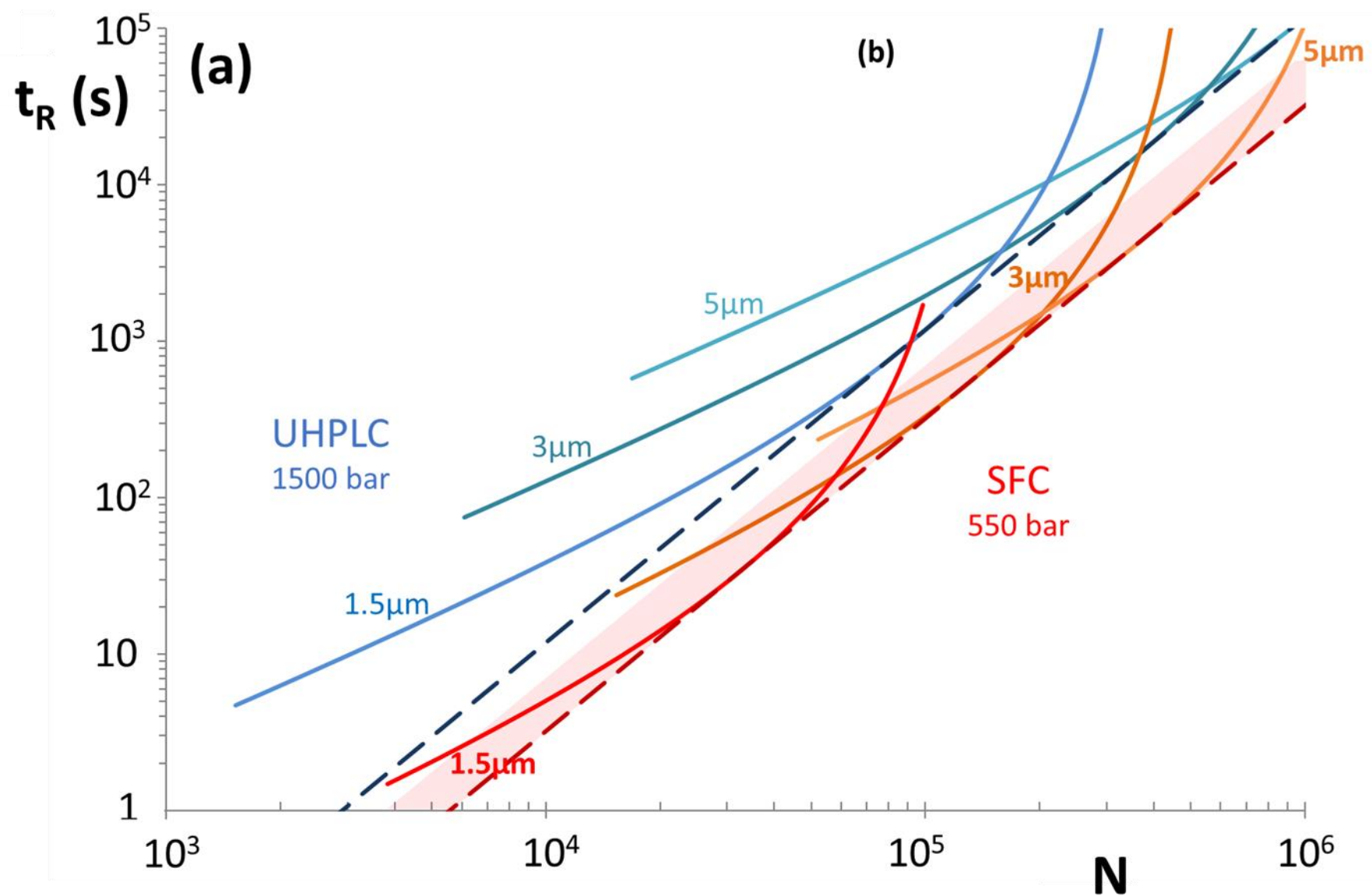
814 [71] B. Lingfeng He, N. G. Kleinsorge, L. Zhang, B. Kleintop, Advancing stereoisomeric separation of
815 an atropisomeric Bruton's tyrosine kinase inhibitor by using sub-2 μm immobilized polysaccharide-
816 based chiral columns in supercritical fluid chromatography, *Journal of Chromatography A* 1626
817 (2020) 461320. <https://doi.org/10.1016/j.chroma.2020.461320>

818 [72] O. Kozlov, K. Kalíková, T. Gondová, M. Budovská, A. Salayová, E. Tesarová, Fast enantioseparation
819 of indole phytoalexins in additive free supercritical fluid chromatography, *Journal of Chromatography*
820 *A* 1596 (2019) 209–216. <https://doi.org/10.1016/j.chroma.2019.03.028>

821 [73] T.A. Berger, Reduced Plate Height of 1.65 on a 20 \times 3 mm Column Packed with 1.8 μm Particles
822 in Supercritical Fluid Chromatography (SFC), *Chromatographia* 82 (2019) 971–974.
823 <https://doi.org/10.1007/s10337-019-03722-z>

- [74] J.J. Heiland, D. Geissler, S.K. Piendl, R. Warias, D. Belder, Supercritical-Fluid Chromatography On-Chip with Two-Photon-Excited-Fluorescence Detection for High-Speed Chiral Separations, *Analytical Chemistry* 91 (2019) 6134–6140. <https://doi.org/10.1021/acs.analchem.9b00726>
- [75] R. De Pauw, K. Choikhet, G. Desmet, K. Broeckhoven, Occurrence of turbulent flow conditions in supercritical fluid chromatography, *Journal of Chromatography A* 1361 (2014) 277–285. <https://doi.org/10.1016/j.chroma.2014.07.088>
- [76] T.A. Berger, Characterizing pressure issues due to turbulent flow in tubing, in ultra-fast chiral supercritical fluid chromatography at up to 580 bar, *Journal of Chromatography A*, 1475 (2016) 86–94. <https://doi.org/10.1016/j.chroma.2016.10.073>
- [77] F. Gritti, Extension of Golay's plate height equation from laminar to turbulent flow I – Theory, *Journal of Chromatography A*, 1492 (2017) 129–135. <http://dx.doi.org/10.1016/j.chroma.2017.02.044>
- [78] F. Gritti, M. Fogwill, Speed-resolution advantage of turbulent supercritical fluid chromatography in open tubular columns: II – Theoretical and experimental evidences, *Journal of Chromatography A*, 1501 (2017) 142–150. <http://dx.doi.org/10.1016/j.chroma.2017.04.032>
- [79] F. Gritti, M. Fogwill, Molecular dispersion in pre-turbulent and sustained turbulent flow of carbon dioxide, *Journal of Chromatography A*, 1564 (2018) 176–187. <https://doi.org/10.1016/j.chroma.2018.06.005>
- [80] F. Gritti, High-resolution turbulent flow chromatography, *Journal of Chromatography A*, 1570 (2018) 135–147. <https://doi.org/10.1016/j.chroma.2018.07.059>
- [81] T.A. Berger, Demonstration of High Speeds with Low Pressure Drops Using 1.8 μm Particles in SFC, *Chromatographia* 72 (2010) 597–602. <https://doi.org/10.1365/s10337-010-1699-2>
- [82] T.A. Berger, Characterization of a 2.6 μm Kinetex porous shell hydrophilic interaction liquid chromatography column in supercritical fluid chromatography with a comparison to 3 μm totally porous silica, *Journal of Chromatography* 1218 (2011) 4559–4568.
- [83] V. Desfontaine, A. Tarafder, J. Hill, J., Fairchild, A. Grand-Guillaume Perrenoud, J-L Veuthey, D. Guillarme, A systematic investigation of sample diluents in modern supercritical fluid chromatography. *Journal of Chromatography A* 1511 (2017) 122–131. <https://doi.org/10.1016/j.chroma.2017.06.075>.
- [84] K.P. de Lima, I.C. Sales Fontes Jardim, M.C. Breitzkreitz, Study of the chromatographic parameters of ultra-high performance supercritical fluid chromatography and method development using a design of experiments approach for the quantification of pesticides in lettuce, *Journal of Separation Science* 41 (2018) 3339–3345.
- [85] M. Sun, C. Turner, M. Sandahl, Signal enhancement in supercritical fluid chromatography-diode-array detection with multiple injection, *Journal of Separation Science* 42 (2019) 3727–3737. <https://doi.org/10.1002/jssc.201900614>
- [86] K. Vanderlinden, G. Desmet, K. Broeckhoven, Effect of the feed injection method on band broadening in analytical supercritical fluid chromatography, *Journal of Chromatography A* 1630 (2020) 461525.

Figure 1:



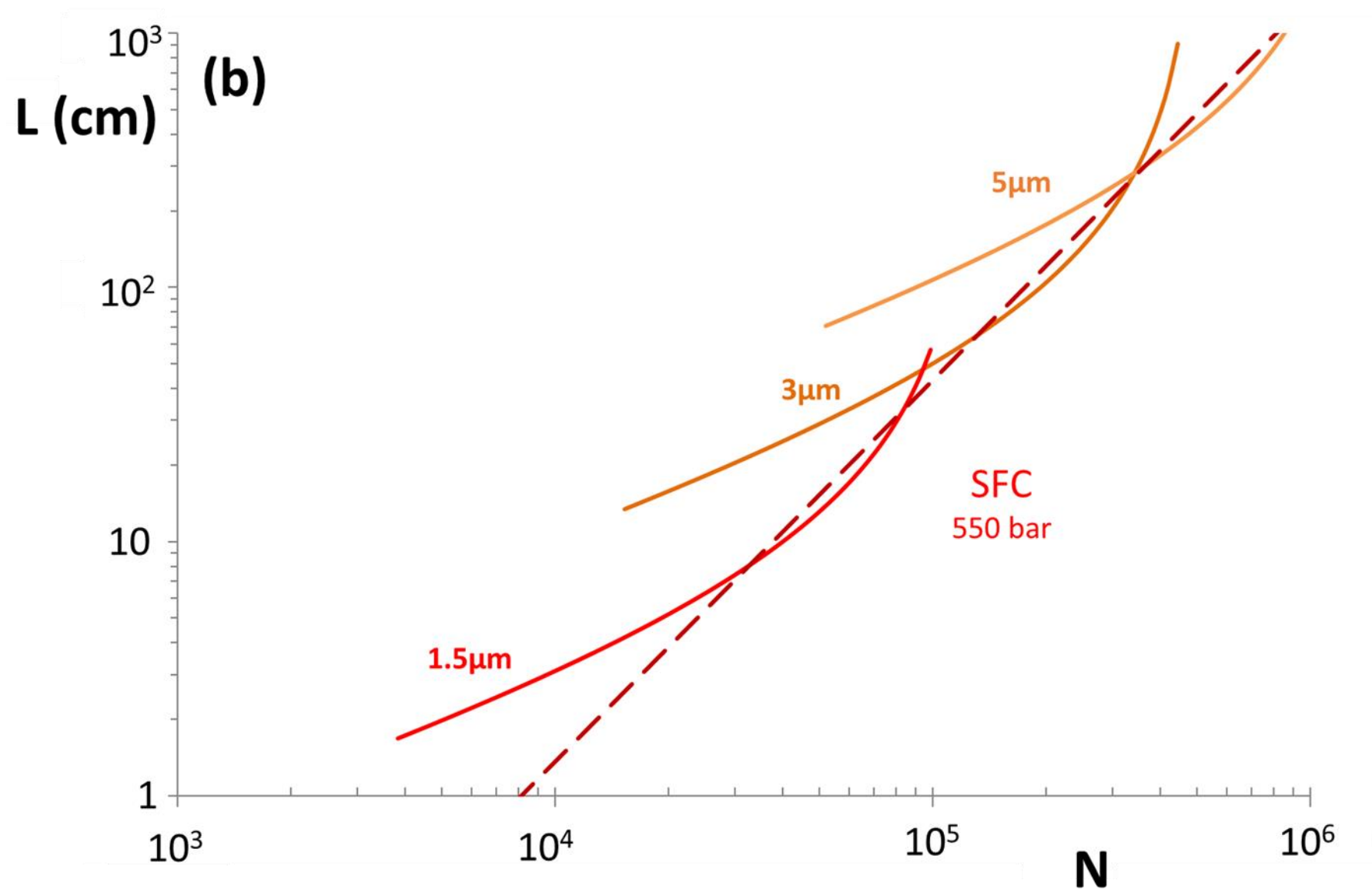


Figure 2:

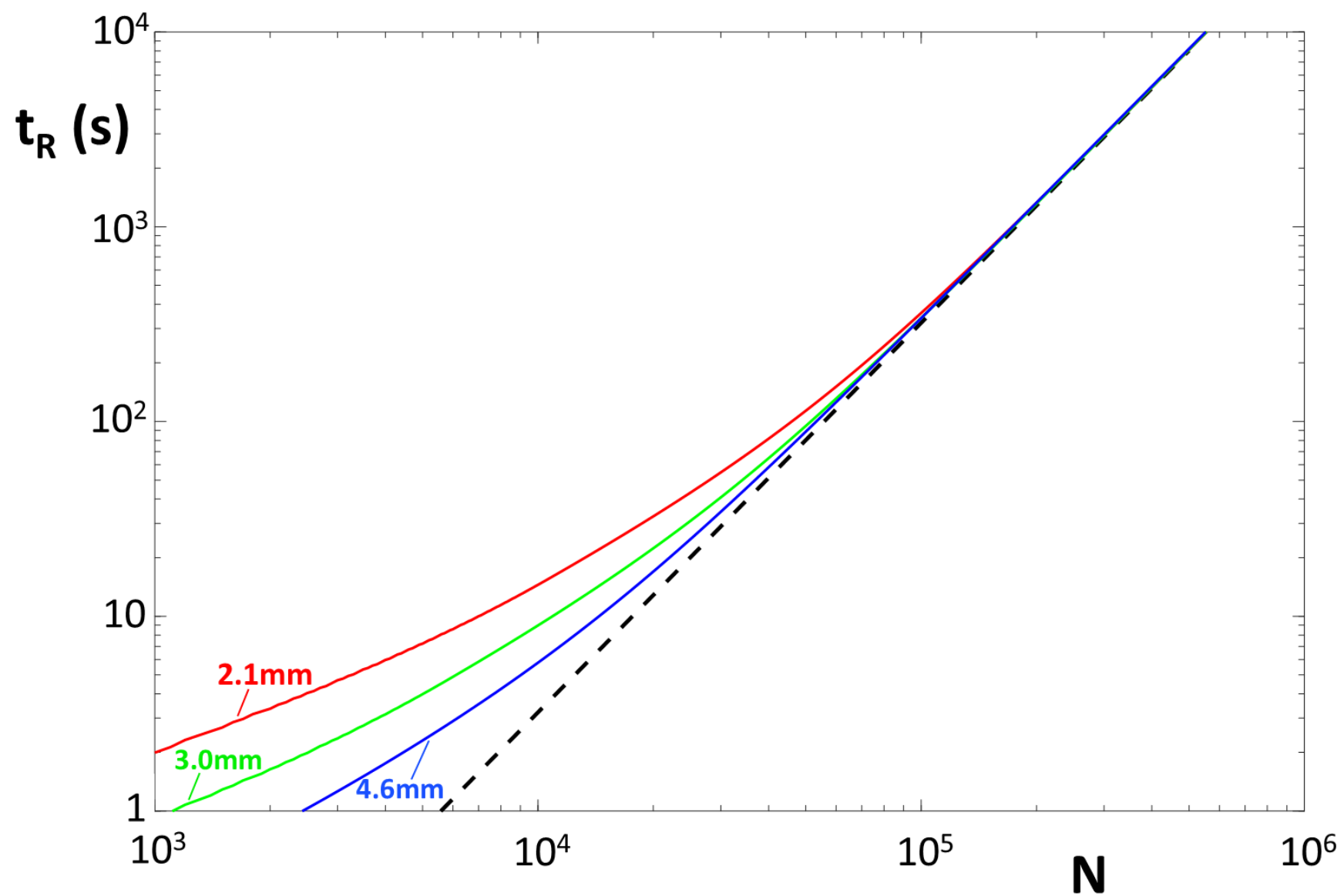


Figure 3:

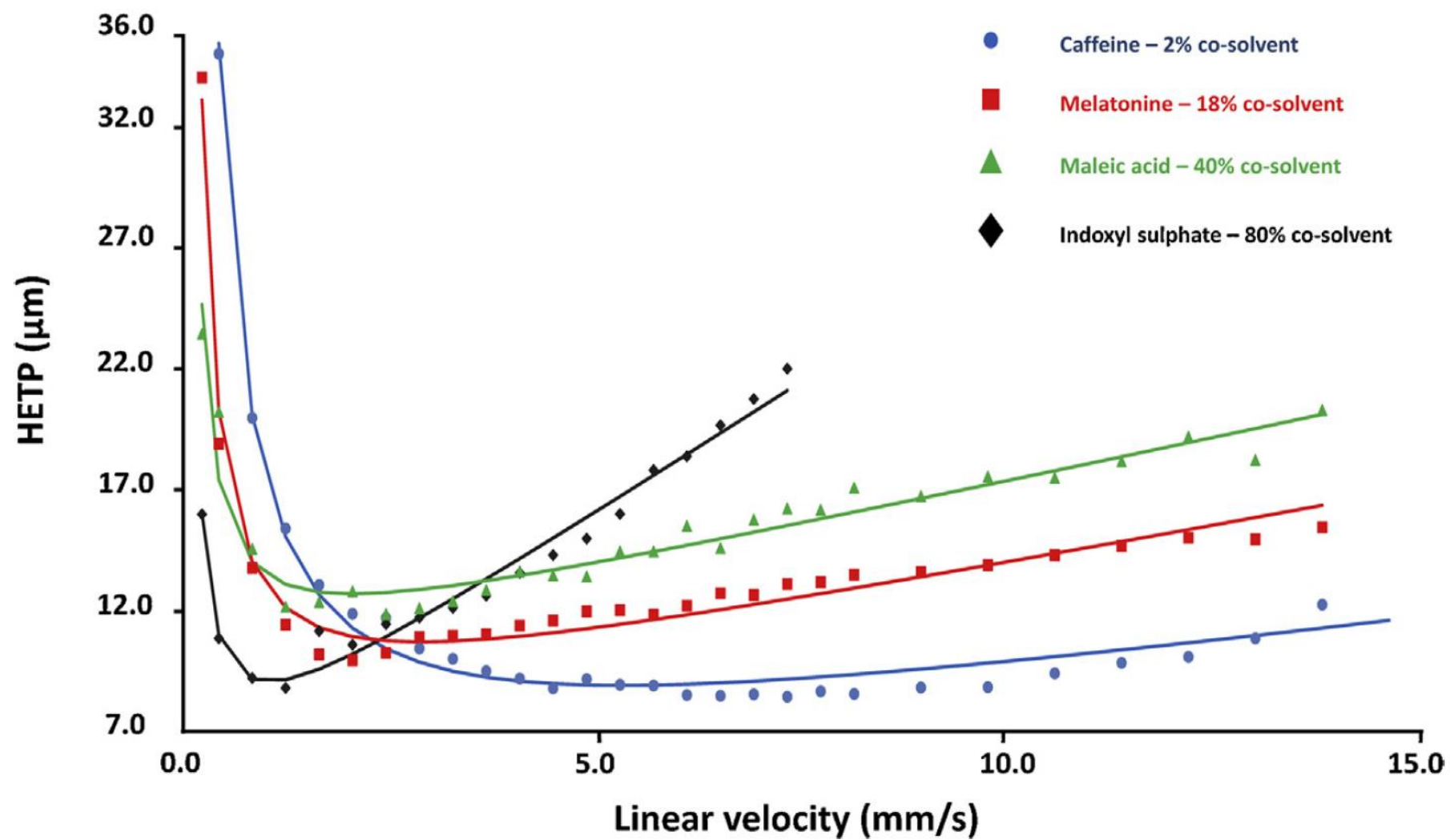


Figure 4:

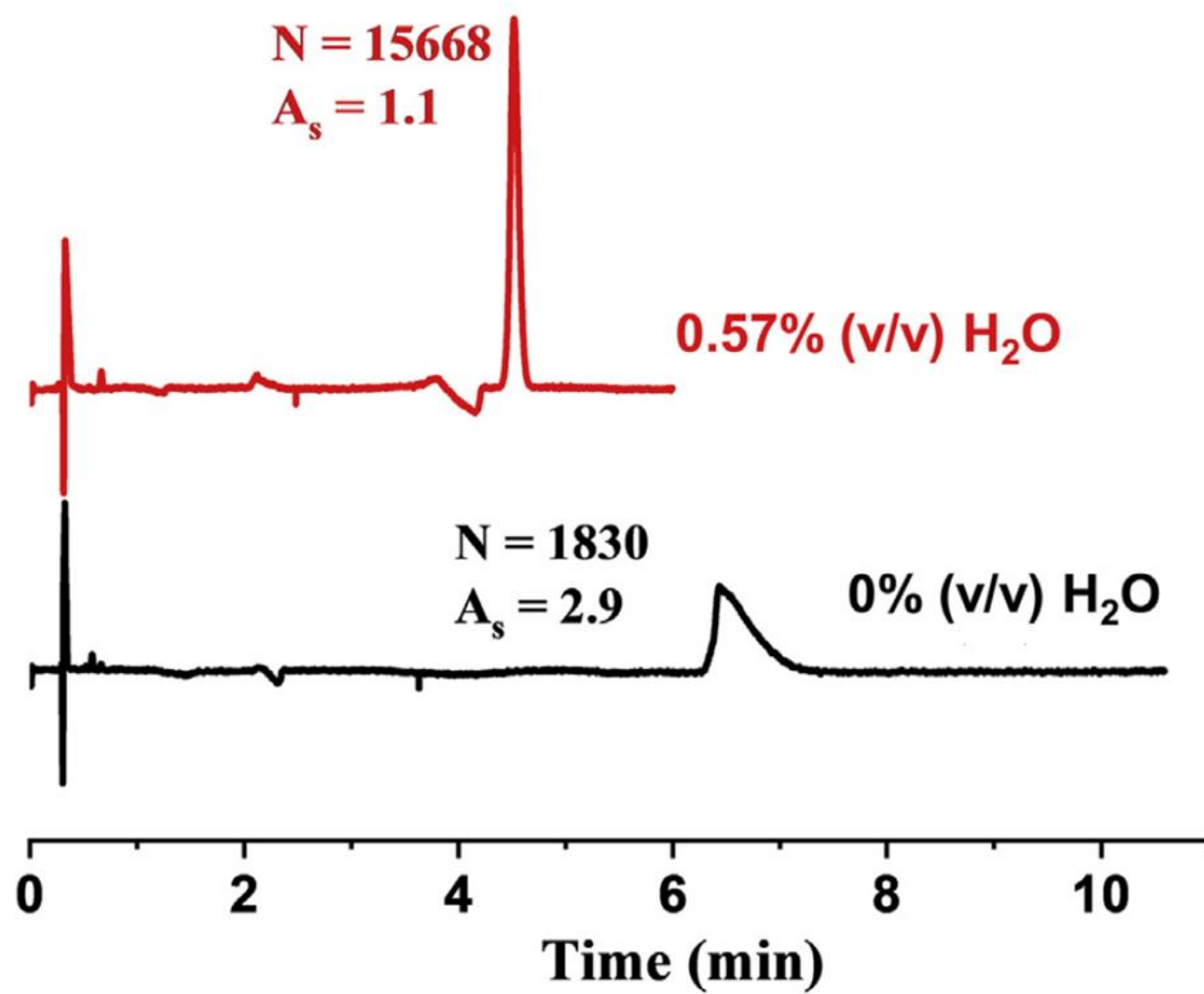


Figure 5:

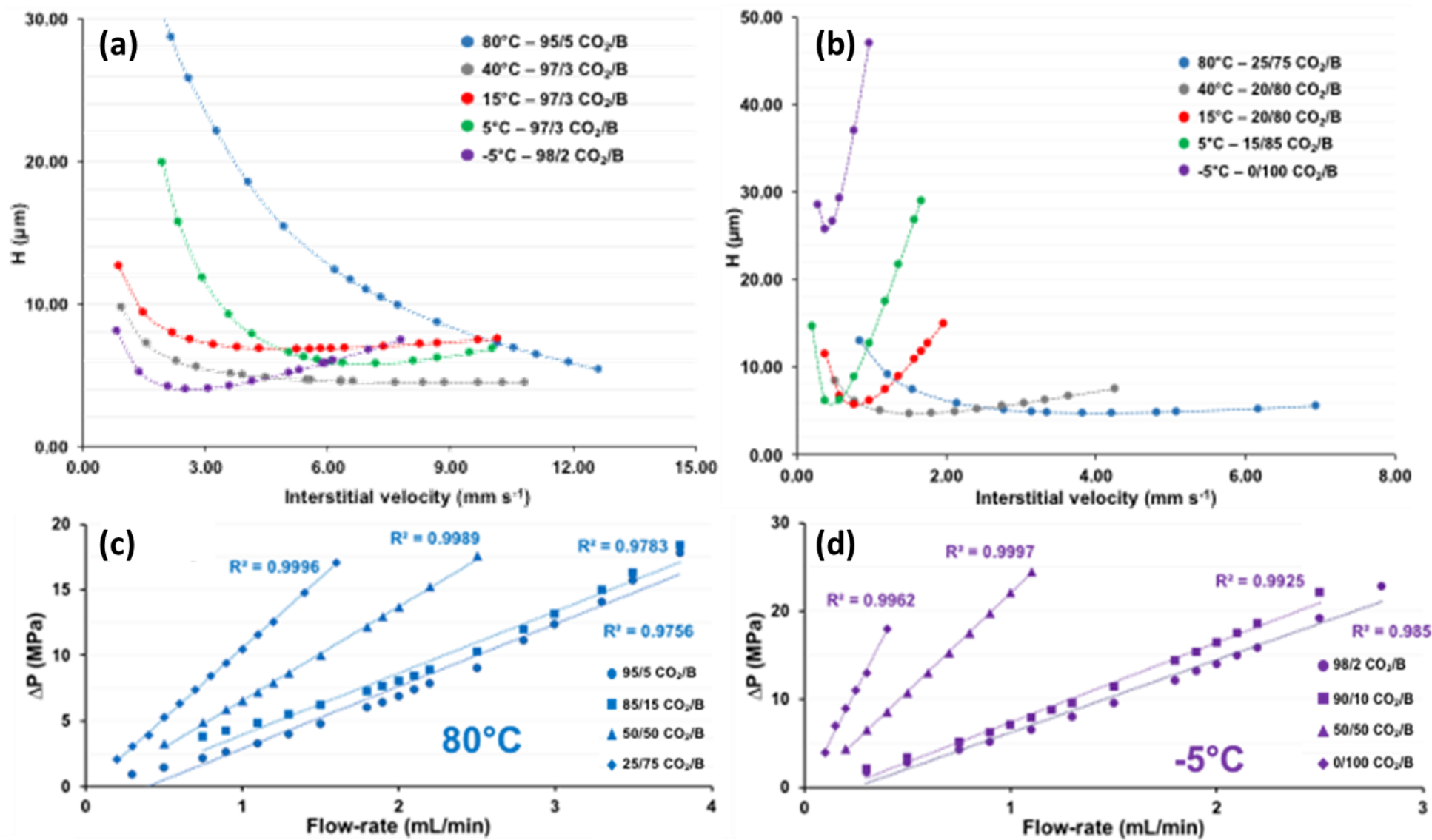


Figure 6:

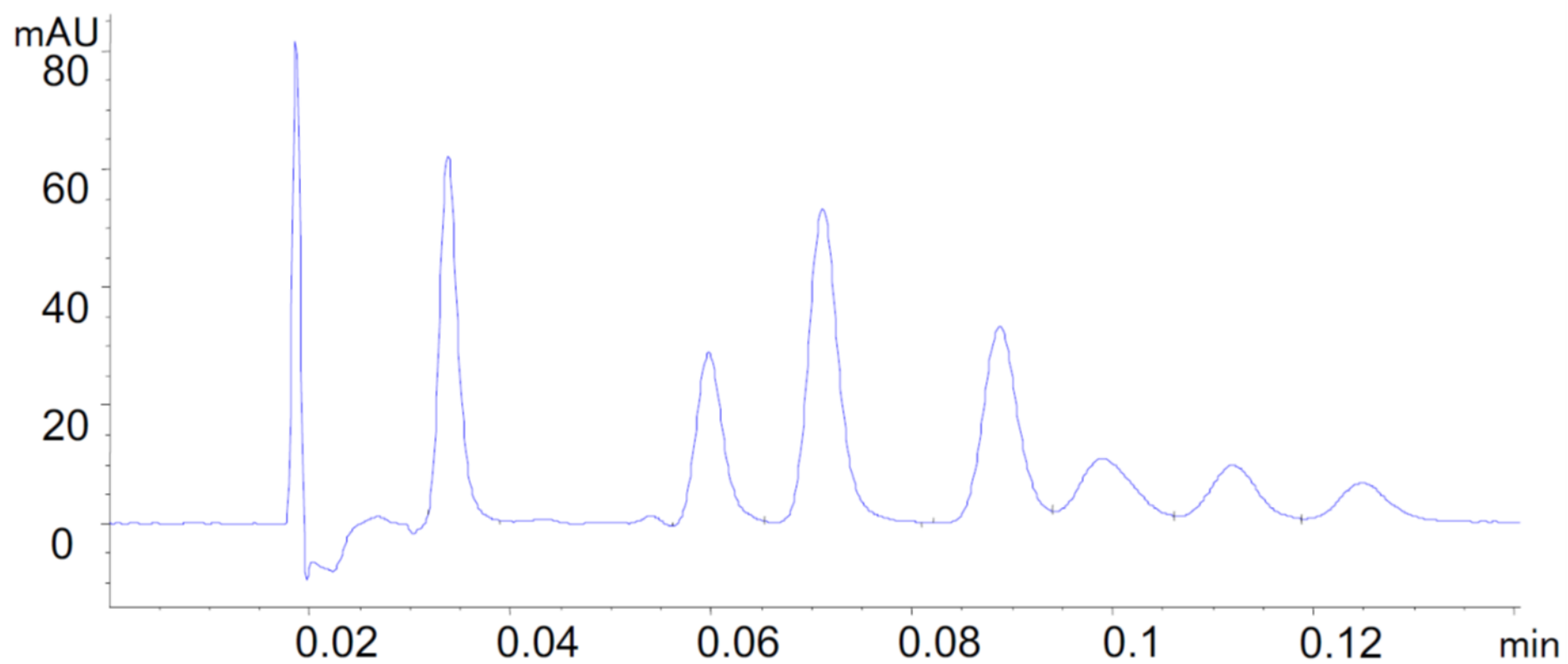


Figure 7:

